

# A hydrogel-based microfluidic device for the studies of directed cell migration†

Shing-Yi Cheng,<sup>a</sup> Steven Heilman,<sup>a</sup> Max Wasserman,<sup>b</sup> Shivaun Archer,<sup>c</sup> Michael L. Shuler<sup>ac</sup> and Mingming Wu<sup>ab</sup>

Received 19th December 2006, Accepted 19th March 2007

First published as an Advance Article on the web 4th April 2007

DOI: 10.1039/b618463d

We have developed a hydrogel-based microfluidic device that is capable of generating a steady and long term linear chemical concentration gradient with no through flow in a microfluidic channel. Using this device, we successfully monitored the chemotactic responses of wildtype *Escherichia coli* (suspension cells) to  $\alpha$ -methyl-DL-aspartate (attractant) and differentiated HL-60 cells (a human neutrophil-like cell line that is adherent) to formyl-Met-Leu-Phe (f-MLP, attractant). This device advances the current state of the art in microchemotaxis devices in that (1) it demonstrates the validity of using hydrogels as the building material for a microchemotaxis device; (2) it demonstrates the potential of the hydrogel based microfluidic device in biological experiments since most of the proteins and nutrients essential for cell survival are readily diffusible in hydrogel; (3) it is capable of applying chemical stimuli independently of mechanical stimuli; (4) it is straightforward to make, and requires very basic tools that are commonly available in biological labs. This device will also be useful in controlling the chemical and mechanical environment during the formation of tissue engineered constructs.

## Introduction

A critical aspect of cell biology is cell migration,<sup>1</sup> which is often mediated by the chemical gradients in the environment.<sup>2,3</sup> For instance, bacteria can sense chemokines and alter its course of random walk to swim up or down the chemokine gradient;<sup>4–6</sup> Neutrophils migrate to specific locations (such as a wound) to perform immune functions when sensing gradients of chemotactic factors such as a bacterial secreted product, formyl-Met-Leu-Phe (f-MLP).<sup>7</sup> Failure of cells to migrate or migration of cells to inappropriate locations can be detrimental to living organisms and can lead to life threatening conditions in the human body. Since cell migration accompanies us from conception to death, and plays important roles in many physiological processes, such as the formation of new tissue, embryogenesis, wound healing, and cancer metastasis, a thorough understanding of the mechanisms underlying cell migration is a critical step for researchers to develop new therapeutic strategies, and for the development of a rational basis for guiding the formation of tissues.

A wide variety of methods have been proposed for chemotaxis assays, including the under-agarose assay,<sup>8</sup>

Boyden chambers (or transwell assays),<sup>9</sup> the Dunn chamber,<sup>10</sup> the Zigmond chamber,<sup>11</sup> and the micropipette-based assay.<sup>7,12</sup> All of these approaches are based on introducing a chemical gradient to the cells of interests, but are often inadequate in providing a reproducible, controllable, and stable linear gradient. Various designs of microfluidic devices have been proposed to address this issue and have been demonstrated for studying chemotaxis in both eukaryotes<sup>13–18</sup> and prokaryotes.<sup>19,20</sup> These devices can be categorized into either flow-based<sup>13,15,17,18,20</sup> or diffusion-based<sup>14,16,19</sup> gradient generators. Flow-based gradient generators have the advantage of establishing the gradient rapidly. A consequence of the flow based gradient generation is that cells are exposed to both the chemical concentration gradient and the shear stresses associated with the flow. This leads to two major problems: (1) it is challenging to separate effects from the shear stresses associated with the flows and the chemical gradient;<sup>21</sup> (2) the fluid flows in these devices immediately carry away any signaling factors (autocrine or paracrine) secreted by the cells that are important in mediating cell migration. Several diffusion-based microfluidic devices were proposed to overcome these issues, these devices are either difficult to fabricate due to their complicated design or are unable to maintain a stable gradient for long-term studies.

The diffusion-based microchemotaxis device developed by Diao *et al.*<sup>19</sup> is the first generation of the device described in this paper. The core of the device is the three adjacent and parallel microfluidic channels fabricated from a piece of 100  $\mu\text{m}$  thick nitrocellulose membrane. A proof of concept experiment was performed using bacterial chemotaxis which demonstrated that the device is capable of generating a linear and steady chemical gradient. However, the device

<sup>a</sup>School of Chemical and Biomolecular Engineering, Cornell University, Ithaca, NY 14853, USA. E-mail: mw272@cornell.edu; Fax: +1 (607) 255-1222; Tel: +1 (607) 254-8319

<sup>b</sup>Sibley School of Mechanical and Aerospace Engineering, Cornell University, Ithaca, NY 14853, USA

<sup>c</sup>Department of Biomedical Engineering, Cornell University, Ithaca, NY 14853, USA

† This paper is part of a special issue 'Cell and Tissue Engineering in Microsystems' with guest editors Sangeeta Bhatia (MIT) and Christopher Chen (University of Pennsylvania).

suffers from several limitations: (1) The device faces run-to-run variations owing to the poor sealing between the nitrocellulose membrane and other components of the device; (2) The choices of chemoattractants are limited due to the poor permeability of proteins through nitrocellulose membrane; (3) There is a long gradient establishing time due to the small diffusion coefficient of nitrocellulose membrane; (4) The channel geometry (width, height) and the distance between channels can not be made precisely due to the fabrication method (nitrocellulose membrane cut by CO<sub>2</sub> laser). To overcome these limitations, we propose a first generation, agarose gel based gradient generator that adapts the concepts of the three channel design in Diao *et al.* (see Fig. 1).

The operation principle of the device is shown in Fig. 1. Three parallel microfluidic channels are patterned on a thin piece of agarose gel (usually less than 1 mm in thickness) through a simple silicon molding process. Fluid flowing in one outer channel (source channel) has a constant chemical concentration, while the fluid flowing in the other outer channel (sink channel) usually is a blank buffer and removes the chemicals in the system. The chemicals diffuse across the channels, and the steady state of the system is a linear chemical concentration gradient in the center channel. This three-channel configuration, diffusion based device has inherent advantages such as the chemical stimuli can be applied independently of mechanical stimuli and the gradient can be maintained indefinitely. There are several other advantages that pertain to using a hydrogel as the diffusion matrix. They are (1) most cell nutrients and growth factors are diffusible in hydrogels, thus a hydrogel-based device can be easily integrated in biological experiments; (2) the diffusivity of most solutes in agarose gels is known to be very close to that in water,<sup>22</sup> so the time required to establish the chemical gradient is short; (3) agarose gel is very malleable, and various feature designs and sizes can be molded onto the agarose gels easily: Whitesides' group have shown that feature sizes as small as 2 μm can be formed on agarose gels;<sup>23</sup> (4) agarose gel is commercially available, non-toxic to the cells and cost effective. Using this assay, we successfully monitored the chemotactic response of a suspension cell line—*Escherichia coli* RP437 and an adherent cell line—differentiated human promyelocytic leukemia cell line, HL-60.

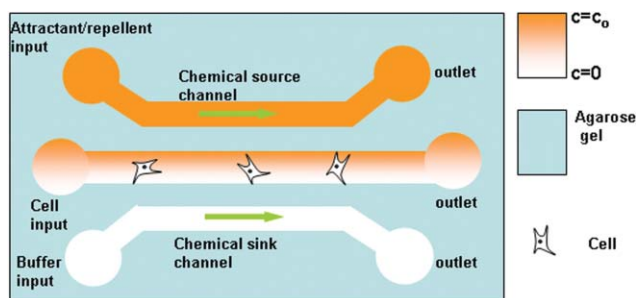


**Fig. 1** Schematics of the three-channel microfluidic device. Solution of a fixed chemical concentration flows in the source channel while blank buffer flows in the sink channel. The chemical diffuses through the agarose gel membrane, and forms a linear gradient in the center channel. The cells are seeded in the center channel.

## Materials and methods

### Fabrication and assembly of devices

The core portion of the chemotaxis device was fabricated with agarose using a standard molding process. The silicon mold with the positive relief features was fabricated using the standard soft lithography technique performed in the Cornell NanoScale Science and Technology Facility. The desired features were designed on L-Edit, converted, exposed, and developed onto a chrome-coated glass mask. A 4 inch diameter silicon wafer was primed with P20 primer (Shipley, Marlborough, MA), and then spin coated with approximately a 4.0 μm thick layer of Shipley 1045 photoresist (Shipley) at 3500 rpm for 1 min. The pattern was then transferred from the mask to the wafer by exposing the wafer to UV light (405 nm wavelength) at 300 mJ cm<sup>-2</sup> using an EV620 contact aligner (Electronic Visions Inc., Phoenix, AZ). The wafer was subsequently developed for 2 min in 300 MIF developer solutions (AZ Electronic Materials, Somerville, NJ). The wafer was etched to a depth of 170 μm in an inductively coupled plasma reactive ion etcher (Unaxis 770, Plasma-Therm Inc., St. Petersburg, FL). The residual photoresist was later removed by acetone and subsequently stripped by oxygen plasma etching (GaSonic Aura 1000 Asher). The silicon master was now ready to be used. The schematic of the pattern on the silicon master is shown in Fig. 2. The width of the three channels is 400 μm. The ridge between center and sink or source channel is 250 μm for all the biological experiments shown below. For calibration purposes, we varied both the center channel width and the ridge width.

A step-by-step procedure for patterning three channels onto agarose gel using the silicon master is illustrated in Fig. 2. (1) A rectangular shaped PDMS ring spacer with a thickness of 225–300 μm, higher than the depth of the channels, was placed around the features on the silicon master to define the overall shape and the thickness of the agarose gel device; (2) A 3% (w/v) aqueous solution (dissolved in phosphate buffered saline buffer (PBS)) of high-gel strength agarose (EMD Chemicals Inc., Darmstadt, Germany) was heated in a microwave oven and the resulting solution was poured onto the area surrounded by the PDMS ring spacer on the silicon master. The agarose solution was quickly pressed down to the same height of the PDMS ring by a glass slide. This step ensured that the agarose gel had a flat surface for proper sealing. The agarose was then allowed to gel at room temperature and ambient pressure; (3) The agarose gel with PDMS ring spacer was peeled off the silicon master and rinsed with DI water. The patterned agarose gel was either stored in PBS for up to a week before being used, or was used straight away; (4) The last step involved sandwiching the agarose gel device between a glass slide and a Plexiglas manifold, and securing the sandwich to a stainless steel support with screws. Care must be taken to ensure that the inlets and outlets of the channels are connected directly to the reservoirs (or access ports) pre-fabricated on the Plexiglas manifold. For detailed descriptions of the Plexiglas manifold, see Diao *et al.*<sup>19</sup> The assembly process varied slightly depending on the cell types used in the experiments. For bacteria experiments or suspension cells, the channel side of the agarose gel was in direct

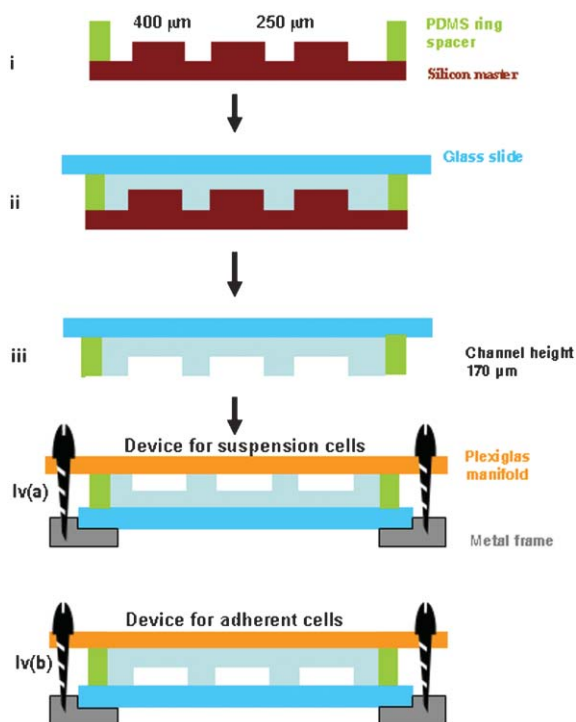


**Fig. 2** Patterning channels on agarose gels. (i) A silicon master is prepared in the Cornell NanoScale Fabrication Center using standard lithography-etching technique. A PDMS ring with thickness higher than the channel depth is put on top of the silicon master around the features. (ii) Hot agarose is poured onto the mold followed by pressing the solution with a glass slide. (iii) The agarose gel is cooled at room temperature, and peeled off with the PDMS ring. The gel is then sandwiched between a glass slide, and a Plexiglas manifold for suspension cells iv(a) and adherent cells iv(b).

contact with the Plexiglas manifold, in this case, the agarose gel was sandwiched between a glass slide and a Plexiglas manifold as shown in Fig. 2 (procedure iv(a)). For HL60 cells or adherent cell types, cell migration occurred on a fibronectin-coated glass slide. Thus, the channel side of the agarose gel needed to be in contact with a fibronectin-coated glass slide so the cells in the center channel could adhere to it. To connect the ports of the Plexiglas manifold to the channels patterned in the agarose gel, sharpened hypodermic needles were used to punch holes through the gel at the inlets and outlets of three channels before the assembly procedure. The device was then sandwiched between a glass slide and a Plexiglas plate as shown in Fig. 2 (procedure iv(b)). To prepare a fibronectin-coated glass slide, the slide was covered with  $50 \mu\text{g ml}^{-1}$  of fibronectin (Sigma, St Louis, MO) for 1 h followed by 0.2% Bovine serum albumin (BSA, Sigma) for 30 min at room temperature and rinsed with Hanks balanced salt solution (HBSS, Gibco, Carlsbad, CA) twice before use.

It should be noted that the fabrication of the silicon master requires specialized facilities. However, once the silicon master is made, it can be transported easily, and can be reused almost indefinitely. In our case, the silicon master has been used more than 100 times, and it is still functioning well. The molding of the hydrogel device and the assembly procedure using the Plexiglas manifold requires tools that are readily available in

any biological laboratory, namely a microwave and screwdrivers. The molding and assembly processes take about 15 minutes, and usually take place just before the cells are ready to be used. This quick and easy to assemble feature is extremely useful when experiments need to be performed in a sterile environment, or when the experiments are in a testing stage where different reagents and cells need to be tried repeatedly.

### Gradient profile calibration

Fluorescein solution (Sigma) was used for visualizing the chemical concentration field in the channels. Initially  $20 \mu\text{l}$  of PBS buffer was added into the inlet of all three channels, and all the excess solution at both the inlets and the outlets of channels was carefully pipetted away in a few minutes. Fluid flow was generated along the side channels with fluorescent dye and blank buffer. The flows in the side channels were gravity driven, their flow rates depended on the difference of fluid level in the inlet and outlet reservoirs. More details are described in our previous publication.<sup>19</sup>  $80 \mu\text{l}$  of  $10^{-4}$  M fluorescein was loaded into the inlet reservoir of the source channel and  $80 \mu\text{l}$  of PBS buffer was loaded into the inlet reservoir of the sink channel. The time when fluorescein/buffer solution was added was set to be  $t = 0$ . To maintain high flow rates in the channels,  $10\text{--}20 \mu\text{l}$  of fluorescein/buffer solution was added into the inlet reservoirs of the source/sink channels respectively every 10–15 min, and excess solutions in the outlet reservoirs of the two channels were carefully pipetted away. We also tested a newer version of the device in which the flows were driven by a syringe pump (Harvard Apparatus, PhD 2000) at a rate of  $5 \mu\text{l min}^{-1}$ . For all the data shown below, we used gravity driven flow. A CCD camera (Cascade 512 B, Photometrics), an inverted fluorescence microscope (Olympus IX51), a FITC filter cube (Chromotechnology Inc.) and a  $4\times$  Olympus objective lens was used to image the fluorescence intensity of all the channels. A typical experiment takes an image every minute for the first ten minutes and every five minutes after that for about one hour. Image J (free software from <http://rsb.info.nih.gov/ij/download.html>) was subsequently used to analyze the data.

### Bacteria chemotaxis experiments

The *E. coli* strain RP437 transformed with plasmid pTrc-GFP, a pTrc99A-based expression vector (Amersham Pharmacia) containing the *gfpmut2* gene downstream from the Trc promoter was used in the bacteria chemotaxis experiment (kindly provided by Dr Matthew DeLisa's laboratory, Cornell University). Cells were grown overnight in 2 ml Luria–Bertani (LB) medium (Fisher, Pittsburgh, PA) supplemented with  $100 \mu\text{g ml}^{-1}$  ampicillin (Sigma) at  $30^\circ\text{C}$  in a 10 ml tube in an incubator shaker. The overnight cultures were then used to inoculate fresh 1.5 ml LB medium supplemented with  $100 \mu\text{g ml}^{-1}$  ampicillin followed by growth at  $30^\circ\text{C}$  in an incubator shaker. To induce the trc promoter controlling the *gfpmut2* gene, isopropyl thiogalactoside (IPTG, Sigma, St Louis, MO) was added into the culture to a final concentration of 1 mM when the optical density at 600 nm ( $\text{OD}_{600}$ ) of the cell culture reached 0.2. After the  $\text{OD}_{600}$  reached 1.0, cells were

centrifuged at 1500 g at room temperature for 2 min, washed with chemotaxis buffer once (PBS/0.1 mM EDTA/1  $\mu$ M methionine/10 mM lactic acid, pH = 7) and centrifuged again at the same speed and time. The resulting pellet was resuspended in chemotaxis buffer.

*E. coli* at a concentration of OD<sub>600</sub> between 1.5 to 2.0 was added into the center channel of the assembled device, and after a few minutes, the excess solutions at the either end of the center channel were removed to stop flow in the center channel. 80  $\mu$ l of chemotaxis buffer and 10<sup>-4</sup>  $\alpha$ -methyl-DL-aspartate (dissolved in chemotaxis buffer) were loaded into the inlet reservoirs of the sink and source channel, respectively. The time when  $\alpha$ -methyl-DL-aspartate was added was set to be  $t = 0$ . Time-lapsed images of the bacterial distribution in the center channel were taken every 30 s by using a 20 $\times$  Olympus objective and the fluorescent imaging system mentioned above.

### HL-60 chemotaxis experiments

HL-60 cells were a gift from Dr Andrew Yen (Cornell University). Cells were cultured in RPMI 1640 (Gibco, Carlsbad, CA) supplemented with 10% heat inactivated FBS (Gibco, Carlsbad, CA) and 1% Penicillin/Streptomycin (Sigma, St Louis, MO) at 37  $^{\circ}$ C with 5% CO<sub>2</sub>. To differentiate HL-60 cells, DMSO (Sigma, St Louis, MO) was added into the cell culture medium to a final concentration of 1.3%.<sup>24</sup> The morphology of the cells started to change from round to more elongated shapes three days after the addition of DMSO. Differentiated cells exposed for 4–7 days to DMSO were used in these experiments. Differentiated HL-60 cells were centrifuged at 1500 rpm for 5 min, then suspended in HBSS buffer. They were centrifuged again at the same speed and time, and finally resuspended in HBSS buffer to a density of 2  $\times$  10<sup>6</sup> cell ml<sup>-1</sup>.

Prior to the start of a chemotaxis experiment, the channels in the assembled device were flushed with 0.2% BSA for 30 min to block any non-specific binding sites and then washed with HBSS buffer twice. The differentiated HL-60 cell solution was added to the center channel of the assembled device and the excess solutions at either ends of the center channel were removed with a pipette. The device was then put in a 5% CO<sub>2</sub>, 37  $^{\circ}$ C incubator for 10–15 min to allow the cells to attach to the fibronectin coated glass slide. The unattached cells were flushed with HBSS buffer. The flow in the center channel was then stopped by removing excess liquid from both ends of the center channel. 80  $\mu$ l of HBSS buffer and 80  $\mu$ l of 250 nM f-MLP (Sigma, St Louis, MO) were loaded into the inlet reservoirs of the sink and source channel, respectively. The time when f-MLP was added was set to be  $t = 0$ . To ensure high flow rates in both the sink and the source channels, 20  $\mu$ l of chemoattractant or buffer were added into the inlet of the source or sink channels every 10 min, and the excess solution in the outlets of the sink and source channels were also carefully removed at the same time. Time-lapsed images of the cells were taken every 15 s using a 10 $\times$  objective for a total length of 45–55 min, a CCD camera (DXC-390, Sony) connected an inverted microscope (MicroOptics IV 900 Series) and the software StreamPix (Norpix, Inc.).

## Results and discussions

### Device characterization

The device characterization is based on an early measurement that the fluorescent light intensity emitted by the fluorescein solution in a microfluidic channel (depth 100  $\mu$ m) recorded using the imaging system (Cascade 512B) is linear to the fluorescein concentration. This linearity holds when the fluorescein concentration is less than 10<sup>-3</sup> M. Based on this information, we chose 10<sup>-4</sup> M fluorescein solution for all the device calibrations. Fig. 3(a) records the fluorescent intensity in all three channels. The fact that the agarose ridges can not be easily discerned in Fig. 3(a) indicates that the diffusivity of the fluorescein in water and in agarose is very similar. This is in agreement with the fact that  $\sim$ 97% of the agarose gel is water. This visual observation is further supported by the linear fluorescence intensity profile across the ridges between the

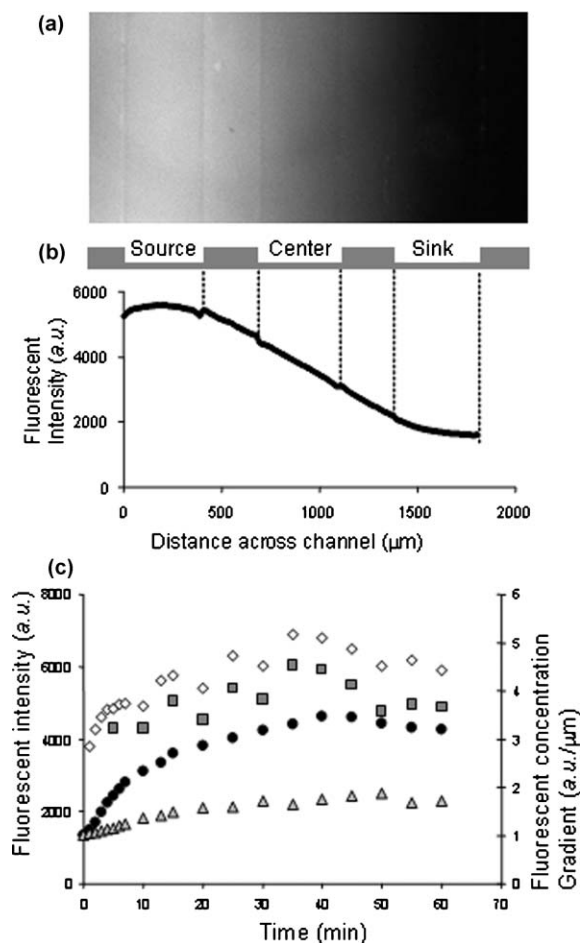


**Fig. 3** (a) Fluorescent intensity of all three channels at  $t = 10$  min. The image is 512 pixel  $\times$  256 pixel, which corresponds to 2048  $\mu$ m  $\times$  1024  $\mu$ m. (b) Fluorescent intensity profile across all three channels using the image in (a). Locations of the channels are indicated. (c) Circles are average fluorescent intensity (proportional to the average chemical concentration  $\bar{C}$ ), and squares are fluorescent intensity gradient (proportional to the chemical concentration gradient  $grad C$ ) as a function of time. Triangles/diamonds represent the average fluorescent intensity in the sink/source channel respectively. Device geometry is described in Fig. 2. The a.u. represents arbitrary units for fluorescent intensity.

sink/source channels and the center channel as shown in Fig. 3(b). It is important to keep the fluorescent intensity constant within either the source or the sink channels for the duration of the experiments; and the gradient was established in the center channel. This is achieved by providing the device with a high enough flow rate in the sink and source channels.

Two important parameters governing the cell migration are the average chemical concentration and the chemical concentration gradient. *Chemokinesis* refers to the cell motility responses to the average chemical concentration; while *chemotaxis* refers to the cell's directed migration under the influence of a chemical gradient. In lieu of this, we measured the average fluorescent intensity (corresponding to average chemical concentration  $\bar{C}$ ) as well as the fluorescent intensity gradient (corresponding to chemical concentration gradient  $grad C$ ) as a function of time (see Fig. 3(c)).

The chemical concentration in the center channel can be described by a one dimensional diffusion equation<sup>25</sup> and the steady solution of the equation gives the chemical concentration gradient  $grad C = C_0/l$ , where  $C_0$  is the chemical concentration in the source channel, and  $l$  is the distance between the source and sink channel. The time  $\tau$  required for the chemical gradient to reach a steady state is  $\tau = l^2/2D$ , where  $D$  is the diffusion coefficient of the chemicals.<sup>25</sup> Here we assume that the agarose gel has the same diffusion coefficient as water, and the system is one dimensional. Fig. 3(c) shows the time evolutions of both average chemical concentration  $\bar{C}$  and gradient  $grad C$  for the device described in Fig. 2. Fig. 3(c) shows that it takes about 10 min to establish a steady chemical gradient; this is consistent with the theoretical estimate that the time for the fluorescein to diffuse through a distance from source channel to sink channel is about  $l^2/2D = 11.2$  min, where  $l = 900 \mu\text{m}$  and  $D = 600 \mu\text{m}^2 \text{s}^{-1}$ . It should be noted that the fluctuations of the fluorescent intensity in the source channel (see diamonds in Fig. 3) are

caused by the manual addition of 20  $\mu\text{l}$  of fluorescent/buffer solution in the source/sink channel every 10 min. This fluctuation can be easily eliminated using a mechanical pump to provide the flow in the source and center channels (data not shown here).

To verify the  $grad C$  dependence on  $l$ , we made three different devices with ridge widths of 250  $\mu\text{m}$ , 125  $\mu\text{m}$  and 50  $\mu\text{m}$ . Using the same experimental procedures described above, all three devices generated a linear gradient. The gradients were 3.4 arbitrary units (a.u.)  $\mu\text{m}^{-1}$  for ridge width 250  $\mu\text{m}$  device, and 4.63 (a.u.)  $\mu\text{m}^{-1}$  for ridge width 125  $\mu\text{m}$  device. Using linear gradient theory, the ratio for the gradients in the 125  $\mu\text{m}$  device and the 250  $\mu\text{m}$  device should be inversely proportional to the distance between the source to sink channel in these two devices, which is  $900 \mu\text{m}/650 \mu\text{m} = 1.38$ , which is in good agreement with our measurements  $4.63/3.4 = 1.36$ . The ridge width 50  $\mu\text{m}$  device did generate a linear gradient, but the measured slope, 3.27 a.u.  $\mu\text{m}^{-1}$ , was much lower than 6.12 a.u.  $\mu\text{m}^{-1}$  predicted by the linear theory. We noticed that the fluorescent intensity across the sink or source channel was not constant in this case. This indicated that a higher flow rate in the source and sink channels was necessary to replenish/remove the chemicals. This problem can be addressed easily by using a mechanical pump. In the experiments described here, we chose to stay with gravity driven flow since the establishing time for the gradient was sufficient for the experiments described below.

## Chemotaxis demonstration

**A. Bacteria chemotaxis experiments.** *E. coli* strain RP437 was loaded into the center channel and chemoattractant  $\alpha$ -methyl-DL-aspartate was loaded into the source channel. Before adding the attractant, cells were randomly distributed in the channel as shown in Fig. 4(a). After the addition of

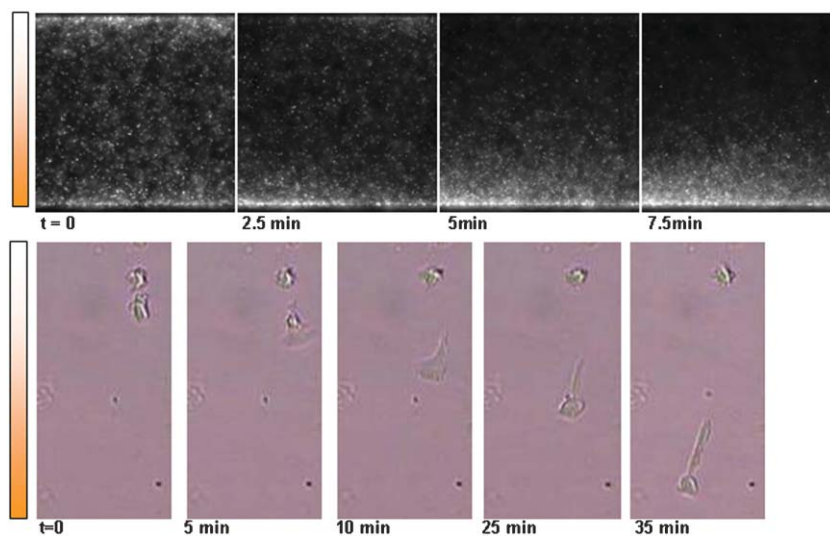


**Fig. 4** Dynamic responses of (a) swimming bacteria (*Escherichia coli*, wildtype RP437) and (b) HL-60 cells to the addition of chemical attractant gradient.  $t = 0$  is defined as the time when attractant and buffer are added to the inlet of the source and sink channels respectively. The temporal evolution of the chemical concentration gradient is shown in Fig. 3(c). The bar on the left is a schematic display of the chemical concentration profile. Each image in (a) is 512 pixel  $\times$  512 pixel, which corresponds to 410  $\mu\text{m}$   $\times$  410  $\mu\text{m}$ . Each image in (b) is 87 pixel  $\times$  171 pixel, which corresponds to an actual size of 102  $\mu\text{m}$   $\times$  200  $\mu\text{m}$ .

$10^{-4}$  M  $\alpha$ -methyl-DL-aspartate into the source channel (corresponding to a final concentration gradient of  $0.111 \mu\text{M} \mu\text{m}^{-1}$ ), cells sensed a change in the chemical environment and migrated towards the higher concentration of attractant and concentrated at the wall closer to the source channel within 10 min (see Fig. 4(a)). Although the duration for which we observed cell motility is shorter than the time required for establishing a stable chemical gradient, the cellular response can be correlated with the temporal evolution of the chemical concentration gradient described in Fig. 3(c). We also performed experiments with  $10^{-5}$  M  $\alpha$ -methyl-DL-aspartate, the characteristic temporal responses of the cells to the chemical gradient is similar to Fig. 4(a). When we used  $10^{-6}$  M  $\alpha$ -methyl-DL-aspartate, no obvious cell migration was observed.

**B. Mammalian chemotaxis experiments.** Human promyelocytic leukemia cell lines, HL-60 cells, were differentiated to neutrophil-like cells by culturing them in 1.3% DMSO culture media for 4–7 days. Cells were washed with and re-suspended in HBSS buffer, and then seeded onto a fibronectin-treated glass that has been assembled in a device as mentioned above. In the absence of the chemical attractant, cells remained stationary. Less than 5 minutes after the addition of 250 nM formyl-Met-Leu-Phe (f-MLP) into the source channel, some cells polarized and started to move. Although the percentage of motile cells in the field of view was small (less than 10%), more than  $\sim 75\%$  of motile cells exhibited chemotactic response, in other words, the majority of motile cells did migrate towards higher concentration of f-MLP. The non-motile cells were likely to be cells that are not fully differentiated, or lack cellular factors that are important for chemotactic response as reported in ref. 27 and 28. Fig. 4(b) shows an adherent HL-60 cell migrating towards high chemo-attractant concentration location. Seen also are the cell morphology changes in the presence of the chemo-attractant. The cell was initially rounded at  $t = 0$ . It later displayed a prominent polar structure with a thin and veil-like protrusions (lamellipodium) at the leading edge, and a tail (uropod) at the rear end of the cells.

We have also tracked the movement of the motile cells in the HL-60 chemotaxis experiments. Fig. 5(a) shows 16 tracked trajectories overlaid on the original image for cells migrating in a chemical gradient of  $0.27 \text{ nM} \mu\text{m}^{-1}$  of f-MLP. The trajectories were obtained from a 1 h long movie using ImageJ software. The random walk nature of the cells is displayed in Fig. 5(b). However, when we plot the unit vector of the total displacement for each of the 16 cells as shown in Fig. 5(c), 12 out of 16 motile cells clearly moved towards the location where f-MLP concentration is higher. We also computed the average persistence length for the 16 cells to be 0.172 along the  $y$  direction (direction of chemical gradient) and 0.0177 along the  $x$  direction (perpendicular to the direction of the chemical gradient). The persistence length is defined as  $\bar{r}/s$ , where  $\bar{r}$  is the displacement vector of the cell trajectory in Fig. 5(a) and  $s$  is the total length that the cell has travelled in 1 h. For a chemical gradient of  $0.54 \text{ nM} \mu\text{m}^{-1}$  f-MLP, the average persistence length was measured to be 0.112 along the  $y$  direction, and 0.055 along the  $x$  direction. This result indicates that the cells are more sensitive to gradient  $0.27 \text{ nM} \mu\text{m}^{-1}$  f-MLP.

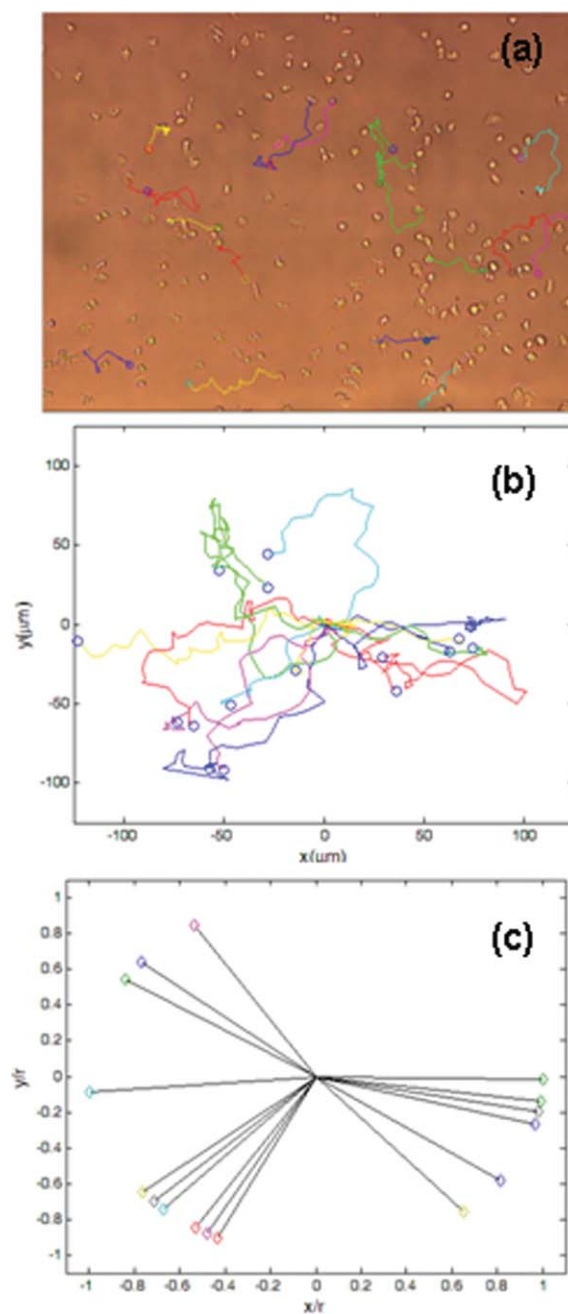


**Fig. 5** (a) Bright field image of HL-60 cells migrating in a  $0.278 \text{ nM} \mu\text{m}^{-1}$  fMLP concentration (low concentration up, high concentration down). The image is  $640 \text{ pixel} \times 480 \text{ pixel}$  which corresponds to  $747 \mu\text{m} \times 562 \mu\text{m}$ . 16 tracks are overlaid on the image, with each colored line a track. The circle marks the end of the track. (b) 16 trajectories re-plotted with each of the track originated at the center. (c) The unit vectors of the 16 tracks shown in (b).

## Concluding remarks

We have developed a first generation hydrogel based micro-chemotaxis device that is suitable for both suspended and adherent cell chemotaxis. We have demonstrated the biocompatibility of the hydrogel based microfluidic device; primarily attributed to the fact that most nutrients and gases necessary for cell survival are readily diffusible in hydrogel. Note that

this is not the case for conventional microfluidic materials such as silicon and PDMS (with the exception of PDMS being permeable to gases). The novel microfluidic platform we have built, hydrogel based microfluidic channels in conjunction with the Plexiglas manifold and steel frame housing, allows for quick assembly of the device (~15 minutes) using commonly accessible tools found in biological labs. In comparison, the assembly of a conventional microfluidic device (PDMS or silicon based) requires non-conventional tools such as a plasma cleaner or anodic bonding machines.

This device can be easily re-configured to suit different applications. For instance, the gradient establishment time can be changed easily by changing the width of the center channel and the ridge between the channels. For our study, we selected 400  $\mu\text{m}$  as the width of the center channel, and 250  $\mu\text{m}$  as the width of the ridge. This channel width was chosen to allow bacteria room to move, since the average swimming velocity of *E. coli* is about 10  $\mu\text{m s}^{-1}$ . For future applications, especially when quick gradient establishment is important, we propose two solutions. One is to decrease the channel and ridge width. For instance, changing the distance between source to sink from 900  $\mu\text{m}$  to 100  $\mu\text{m}$  will decrease the gradient establishment time to about ~10 s. The other approach is to use photocaged chemicals that have previously been used to study bacterial chemotaxis.<sup>26</sup> It is known that caged chemicals can be released in a few milliseconds when exposed to ultraviolet light flashes. By incorporating photocaged chemicals in our device, we can easily establish a chemo-attractant concentration gradient within a few milliseconds. This feature is important for the studies of bacterial chemotaxis, since the bacteria respond to chemo-attractant in a few seconds.

Differentiated HL-60 cells were used as an example to demonstrate the capabilities of this device for studying adherent cell migration. Although migration behaviors of DMSO differentiated HL-60 cell has been shown to be similar to that of primary neutrophils, we have observed, as well as reported by others,<sup>27,28</sup> that only a small population of these cells are motile. Nonetheless, a high percentage of motile cells showed a chemotactic response, and we clearly saw the typical characteristics of migrating cells on a 2D substrate: a prominent polar structure of thin, veil-like protrusions (lamellipodium) at the leading edge and a tail (uropod) that is pulled along at the rear end of the cells.

This device (slightly modified in its design) is currently being used to provide a controlled chemical and mechanical environment for the formation of a 3D microvascular tissue construct using endothelial cells (human umbilical vein endothelial cells) and a collagen matrix. The mechanical environment is generated by the shear stresses of the fluid flow in the center channel where cells reside, as well as the pressure differences between the inlet and outlet of the center channel. The hydrogel based microfluidic device proves to be extremely useful when conducting such long term experiments, since nutrients and gases necessary for cell survival are readily diffusible through the hydrogel from the side channels.

## Acknowledgements

The authors wish to thank Dr Andrew Yen for providing HL-60 cells, Dr Parkinson for providing bacterial strains (RP437), Dr Matthew DeLisa for providing GFP bacterial strains (RP437), and Dr Peng Zhou for helpful discussions. This work was supported, in part, with funds from the National Science Foundation (CBET-0619626), the New York State Office of Science, Technology and Academic Research (NYSTAR) (in the form of a Center for Advanced Technology grant), and the Nanobiotechnology Center (NBTC), an STC Program of the National Science Foundation under Agreement No. ECS-9876771. Part of this work was performed at the Cornell NanoScale Facility, a member of the National Nanotechnology Infrastructure Network, which is supported by the National Science Foundation (Grant ECS 03-35765).

## References

- 1 S. Li, J. L. Guan and S. Chien, *Annu. Rev. Biomed. Eng.*, 2005, **7**, 105.
- 2 P. J. Van Haastert and P. N. Devreotes, *Nat. Rev. Mol. Cell Biol.*, 2004, **5**, 626.
- 3 C. A. Parent and P. N. Devreotes, *Science*, 1999, **284**, 765.
- 4 V. Sourjik, *Trends Microbiol.*, 2004, **12**, 569.
- 5 G. H. Wadhams and J. P. Armitage, *Nat. Rev. Mol. Cell Biol.*, 2004, **5**, 1024.
- 6 H. C. Berg, *Annu. Rev. Biophys. Bioeng.*, 1975, **4**, 119.
- 7 G. Servant, O. D. Weiner, P. Herzmark, T. Balla, J. W. Sedat and H. R. Bourne, *Science*, 2000, **287**, 1037.
- 8 B. Heit and P. Kubes, *Sci. STKE*, 2003, **2003**, PL5.
- 9 S. Boyden, *J. Exp. Med.*, 1962, **115**, 453.
- 10 D. Zicha, G. A. Dunn and A. F. Brown, *J. Cell Sci.*, 1991, **99**(Pt 4), 769.
- 11 S. H. Zigmond, *J. Cell. Biol.*, 1977, **75**, 606.
- 12 K. Wong, O. Pertz, K. Hahn and H. Bourne, *Proc. Natl. Acad. Sci. U. S. A.*, 2006, **103**, 3639.
- 13 D. Irimia, S. Y. Liu, W. G. Tharp, A. Samadani, M. Toner and M. C. Poznansky, *Lab Chip*, 2006, **6**, 191.
- 14 C. W. Frevert, G. Boggy, T. M. Keenan and A. Folch, *Lab Chip*, 2006, **6**, 849.
- 15 F. Lin and E. C. Butcher, *Lab Chip*, 2006, **6**, 1462.
- 16 V. V. Abhyankar, M. A. Lokuta, A. Huttenlocher and D. J. Beebe, *Lab Chip*, 2006, **6**, 389.
- 17 S. Koyama, D. Amarie, H. A. Soini, M. V. Novotny and S. C. Jacobson, *Anal. Chem.*, 2006, **78**, 3354.
- 18 N. Li Jeon, H. Baskaran, S. K. Dertinger, G. M. Whitesides, L. Van de Water and M. Toner, *Nat. Biotechnol.*, 2002, **20**, 826.
- 19 J. Diao, L. Young, S. Kim, E. A. Fogarty, S. M. Heilman, P. Zhou, M. L. Shuler, M. Wu and M. P. DeLisa, *Lab Chip*, 2006, **6**, 381.
- 20 H. Mao, P. S. Cremer and M. D. Manson, *Proc. Natl. Acad. Sci. U. S. A.*, 2003, **100**, 5449.
- 21 G. M. Walker, J. Sai, A. Richmond, M. Stremler, C. Y. Chung and J. P. Wikswo, *Lab Chip*, 2005, **5**, 611.
- 22 E. J. Schantz and M. A. Lauffer, *Biochemistry*, 1962, **1**, 658.
- 23 M. Mayer, J. Yang, I. Gitlin, D. H. Gracias and G. M. Whitesides, *Proteomics*, 2004, **4**, 2366.
- 24 S. J. Collins, F. W. Ruscetti, R. E. Gallagher and R. C. Gallo, *Proc. Natl. Acad. Sci. U. S. A.*, 1978, **75**, 2458.
- 25 H. C. Berg, *'Random Walks in Biology'*, Princeton University Press, 1993.
- 26 R. Jasuja, Y. Lin, D. R. Trentham and S. Khan, *Proc. Natl. Acad. Sci. U. S. A.*, 1999, **96**, 11346.
- 27 W. H. Meyer and T. H. Howard, *Blood*, 1987, **70**, 363.
- 28 J. A. Fontana, D. G. Wright, E. Schiffman, B. A. Corcoran and A. B. Deisseroth, *Proc. Natl. Acad. Sci. U. S. A.*, 1980, **77**, 3664.